Influence of Transition Rates and Scan Rate on Kinetic Simulations of Differential Scanning Calorimetry Profiles of Reversible and Irreversible Protein Denaturation†

James R. Lepock,* Kenneth P. Ritchie, Michael C. Kolios, A. Michael Rodahl, Karl A. Heinz, and Jack Kruuv

Guelph-Waterloo Program for Graduate Work in Physics, Waterloo Campus, University of Waterloo, Waterloo, Ontario N2L 3G1, Canada

Received July 9, 1992; Revised Manuscript Received October 2, 1992

ABSTRACT: The thermodynamic parameters characterizing protein folding can be obtained directly using differential scanning calorimetry (DSC). They are meaningful only for reversible unfolding at equilibrium, which holds for small globular proteins; however, the unfolding or denaturation of most large, multidomain or multisubunit proteins is either partially or totally irreversible. The simplest kinetic model describing partially irreversible denaturation requires three states:

$$N \underset{k_2}{\overset{k_1}{\rightleftarrows}} U \xrightarrow{k_3} D$$

We obtain numerical solutions for N, U, and D as a function of temperature for this model and derive profiles of excess specific heat (C_p) in terms of the reduced variables v/k_i and k_1/k_3, where v is the scan rate. The three-state model reduces to the two-state reversible or irreversible models for very large or very small values of k_1/k_3, respectively. The apparent transition temperature (T_{app}) is always reduced by the irreversible step (U → D). For all values of k_3, T_{app} is independent of v/k_1 at sufficiently slow scan rates, even when denaturation is highly irreversible, but increases identically for all models at fast scan rates in which case the excess specific heat profile is determined by the rate of unfolding. Accurate values of ΔH and ΔS can be obtained for the reversible step only when k_1 is more than 2000–50 000 times greater than k_3. In principle, approximate values for the ratio k_1/k_3 can be obtained from plots of fraction unfolded vs fraction irreversibly denatured as a function of temperature; however, the fraction irreversibly denatured is difficult to measure accurately by DSC alone. A guide to determining whether a reversible analysis is appropriate for analyzing DSC scans for apparently irreversible denaturation is described on the basis of these plots. While a high level of irreversibility can be tolerated at greater than 95% unfolding, at lower levels of unfolding only very low levels of irreversibility (1–14% at 75% unfolding and less than 2% at 50% unfolding) can occur for accurate determination of ΔH and ΔS and deconvolution of complex profiles using models that assume reversibility. Under conditions of higher irreversibility, a kinetic analysis is both more appropriate and more informative.

Differential scanning calorimetry (DSC) is a useful tool for studying the unfolding of proteins as a means of gaining information about protein folding and stability (Privalov, 1989; Dill et al., 1989), domain structure and interaction (Privalov, 1982; Brandts et al., 1989), and ligand binding (Robert et al., 1989). Profiles are obtained of excess specific heat (C_p) as a function of temperature after correction for the difference in C_p (ΔC_p) between the native and denatured states. For simple reversible unfolding (N ⇄ U), the thermodynamic parameters ΔH, ΔS, and ΔH_{cal} can be obtained directly by fitting the profile using the van't Hoff equation as long as N and U are in equilibrium. Methods also have been developed for fitting and deconvoluting multistep transitions of the form N ⇄ I_1 ⇄ I_2 ⇄ ... ⇄ U to obtain the thermodynamic parameters for each step (Biltonen & Freire, 1978; Privalov & Filimonov, 1977; Kidokuro & Wada, 1987). Deconvolution permits monitoring of the unfolding of discrete domains from which a model of domain organization and interactions can be developed (Tsalkova & Privalov, 1985).

The thermal inactivation and denaturation of many proteins are irreversible under the conditions used to measure thermal denaturation in aqueous solutions and have been modeled for the two-state case of $N \xrightarrow{k} D$; however, ΔH and ΔS are not meaningful for an apparently irreversible process since the native and denatured species cannot be at equilibrium. An analytical solution for N and D as a function of temperature can be obtained by solution of the temperature integral $\int e^{-E/RT}\,dT$ (Popescu et al., 1986) which can only be done by approximate methods (Fujita et al., 1979; Sánchez-Ruiz et al., 1988; Lepock et al., 1990a).

The denaturation of most proteins falls into neither of these extreme cases but is partially reversible under most conditions. In addition, nearly all proteins denature irreversibly if held at 90–100 °C for 1–2 h, even if unfolding occurs at a much lower temperature (Zale & Klibanov, 1986). The simplest model that is consistent with these observations is a reversible unfolding followed by an irreversible process:

$$N \underset{k_2}{\overset{k_1}{\rightleftarrows}} U \xrightarrow{k_3} D$$

which locks the unfolded protein in a state from which it cannot refold over the time of the experiment. This may be

† Supported by USPHS Grant CA40251 awarded by the National Cancer Institute, DHHS, to J.R.L. and by grants from the Natural Sciences and Engineering Council of Canada.

* Address correspondence to this author at the Department of Physics, University of Waterloo, Waterloo, Ontario N2L 3G1, Canada.

0006-2960/92/0431-12706$03.00/0

due to aggregation, improper disulfide bond formation, or covalent alterations (Zale & Klibanov, 1986).

Deconvolution and curve fitting of DSC profiles of proteins which undergo apparently irreversible denaturation are commonly done using an equilibrium thermodynamic analysis and predictions made of specific models of domain organization and interaction. It has been argued that this analysis is proper if $k_3 \ll k_1$ over the range of the transition (Sturtevant, 1987; Edge et al., 1988). This is equivalent to the lack of formation of significant amounts of irreversibly denatured protein over the region of the DSC profile of C_p vs temperature from which information is extracted. However, if $k_3 \gtrsim k_1$, a kinetic analysis explicitly considering the rate constant for irreversibility is required.

If the rates of unfolding and folding are explicitly considered, it is possible to obtain kinetic information by calorimetry for some proteins which reversibly unfold (Mayorga & Freire, 1987; Freire et al., 1990). In addition, a three-state model in which the first step of unfolding is treated by equilibrium thermodynamics and the second, irreversible step by kinetics has been investigated (Freire et al., 1990). Sánchez-Ruiz (1992) has performed a theoretical analysis using this model including ligand binding and monomer dissociation to show that irreversibility can significantly perturb the shape of DSC profiles so that under some conditions the extraction of thermodynamic information is not possible. However, the fully kinetic model in which each step of unfolding, refolding, and irreversibility is treated in terms of the rate of that process has not been examined. This is important since a kinetic analysis is necessary if the scan rate approaches the rates of unfolding and refolding even for completely reversible unfolding. This occurs for the rapidly refolding ribonuclease A at fast scan rates (Mayorga & Freire, 1987) and is likely at slower scan rates for large multidomain and multisubunit proteins.

We give the general differential equations for the kinetic three-state model of irreversible denaturation, solve them numerically, and express the results (excess C_p vs T) in terms of k_1, k_2, k_3, and the scan rate v. Two-state reversible and irreversible denaturations are shown to be special cases of the three-state model. The effect of scan rate and the relative values of the rate constants on the DSC profiles are given. In particular, the range of the ratio k_1/k_3 over which reversible curve fitting and deconvolution based on reversible unfolding are appropriate is determined, and an approximate expression of this in terms of the fraction of protein irreversibly denatured during the scan is given. These results are expressed in the form of DSC profiles (excess C_p vs T). However, since C_p is proportional to the temperature derivative of the fraction unfolded, these results are applicable to any procedure by which unfolding or denaturation is measured as a function of temperature varied uniformly with time (e.g., fluorescence, CD, etc.).

MATERIALS AND METHODS

The kinetic equation

$$\mathrm{N} \underset{k_2}{\overset{k_1}{\rightleftarrows}} \mathrm{U} \xrightarrow{k_3} \mathrm{D}$$

where N is the native species, U the reversibly unfolded intermediate, and D the irreversibly denatured form is described by the set of differential equations:

$$dN/dt = -k_1N + k_2U \quad (1)$$

$$dU/dt = k_1N - k_2U - k_3U \quad (2)$$

$$dD/dt = k_3U \quad (3)$$

These give the change in the concentration of N, U, and D as a function of time at constant temperature. The temperature dependence of k can be approximated by the Arrhenius relation. Thus

$$k_i(T) = e^{A_i - E_i/RT}$$

where E_i is the activation energy, which gives the temperature dependence, and A_i the frequency factor. During a DSC scan, temperature (T) varies uniformly with time (t) and can be written as $T(t) = T_0 + vt$. Substitution of the explicit forms of k_i and T into eq 1–3 gives the following set of nonlinear differential equations:

$$dN/dt = -e^{\alpha_1}N + e^{\alpha_2}U$$

$$dU/dt = e^{\alpha_1}N - e^{\alpha_2}U - e^{\alpha_3}U$$

$$dD/dt = e^{\alpha_3}D$$

where $\alpha_i = A_i - E_i/[R(T_0 + vt)]$. An exact, analytical solution for N, U, and D as a function of time and temperature is not possible. The equations for the reversible

$$\mathrm{N} \underset{k_2}{\overset{k_1}{\rightleftarrows}} \mathrm{U}$$

$$dN/dt = -e^{\alpha_1}N + e^{\alpha_2}U$$

$$dU/dt = e^{\alpha_1}N - e^{\alpha_2}U$$

and irreversible

$$\mathrm{N} \xrightarrow{k_1} \mathrm{D}$$

$$dN/dt = -e^{\alpha_1}N$$

two-state models were generated similarly, and the equations for the three models were solved by standard numerical methods for a range of values of k_1, k_2, k_3, and v.

The fractional concentration of each component (N, U, and D) is expressed as a function of temperature. These results can be most generally described by a transition temperature. Three definitions of the transition temperature are used: T_m, the equilibrium transition temperature (the temperature at which $N = U$); T_{app}, the measured transition temperature when the system is not at equilibrium ($N = N_0/2$ but $N \neq U$); T_{max}, the temperature at which the excess C_p is a maximum.

The rate of transition between the states N, U, and D is determined by the free energy of activation ($\Delta G^\ddagger$). The value of $\Delta G^\ddagger$ for each transition is given by $\Delta G^\ddagger_i = E_i - RA_iT$ and the free energy difference between N and U by $\Delta G = E_2 - RA_2T - \Delta G^\ddagger_1$. The E_i's and A_i's were selected by setting $\Delta H = 400$ kJ/mol and $\Delta S = 1319.5$ J K^{-1} mol^{-1} for the reversible step N $\rightleftarrows$ U. The value of $\Delta H = 400$ kJ/mol is an average value for the unfolding of a number of small, globular proteins (Privalov & Khechinashvili, 1974). ΔH varies with temperature, and the actual temperature dependence of ΔH for denaturation of chymotrypsinogen (Brandts, 1964) was used with only a small effect on the profile of C_p vs T and the final calculations (results not shown). These values give a transition temperature T_m of 30 °C. The T_m selected is arbitrary and can be varied by changing A_1 slightly with no effect on the final results. Since the equilibrium constant (K_{eq}) can be

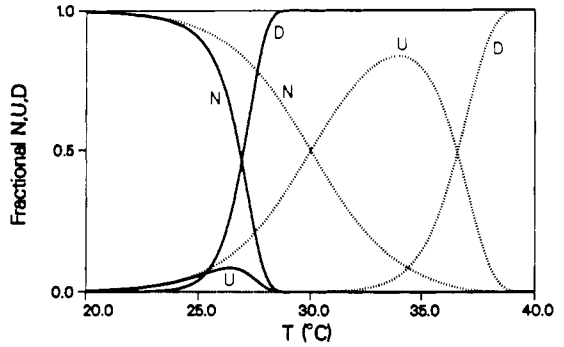

FIGURE 1: Fractional populations of the native (N), reversibly unfolded (U), and irreversibly denatured (D) states as a function of temperature for three-state denaturation. The ratio of the scan rate (v) to k_1 at 30 °C (the T_m for reversible denaturation) is 0.01, and $v/k_3 = 0.01$ (solid lines) and 500 (dashed lines), giving values of k_1/k_3 at T_m of 1 and 5×10^4, respectively.

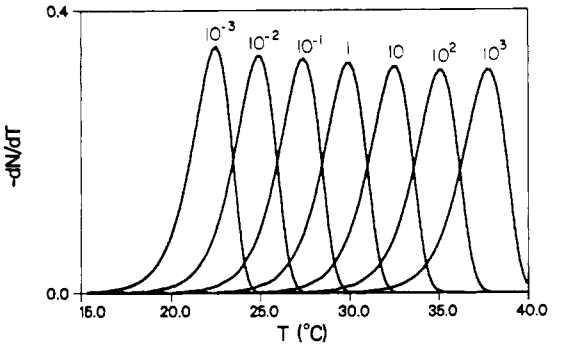

FIGURE 2: DSC profiles for two-state irreversible denaturation for $v/k_1 = 0.001$–1000 at 30 °C.

expressed as

$$K_{eq} = U/N = k_1/k_2 = e^{-\Delta G/RT}$$

the Arrhenius constants obey the relations

$$E_1 - E_2 = \Delta H$$

$$A_1 - A_2 = \Delta S/R$$

for reversible, two-state unfolding.

It is clear from the above equations that E_1 must be greater than ΔH. The value of E_1 was set at 685 kJ/mol, which sets E_2 at 185 kJ/mol, and A_1 was selected to give the desired k_1 at T_m = 30 °C. This fixes k_2 and A_2 since $k_1/k_2 = 1$ at T_m. The value of E_3 was also set to 685 kJ/mol, and A_3 was varied to obtain the desired value of k_3 at 30 °C.

The activation energy of 685 kJ/mol used for E_1 and E_3 is similar to that found for the irreversible inactivation of the Ca^{2+}-ATPase of rabbit sarcoplasmic reticulum (Lepock et al., 1990a). This is an apparent inactivation rate constant which is a function of k_1, k_2, and k_3 if, as is likely, the two-state model of irreversible inactivation is actually an approximation of the three-state model with $k_3 \gtrsim k_1$. If this is true, then the reversible unfolding is the rate-limiting step, and the activation energy for irreversible inactivation should approximate the activation energy of unfolding. Thus, 685 kJ/mol was chosen for E_1. The same value was used for E_3 for simplicity. The specific values of E_i and A_i are important since they define the denaturation process and the shape of the DSC profile, and they obviously vary for different proteins; however, the main conclusions of this work do not depend on the specific values of E_i and A_i used.

The fractional values of N, U, and D were calculated as a function of temperature. The total enthalpy change was assumed to occur during the first, reversible step. Thus, the excess specific heat [$C_p(T)$] is given by

$$C_p \propto -(dN/dT)$$

The best fit of the curves of C_p vs temperature was determined using the Simplex minimization algorithm assuming either two-state irreversible denaturation as previously described (Lepock et al., 1990) or two-state reversible denaturation where

$$K_{eq} = U/N = e^{\Delta S/R - \Delta H/RT}$$

RESULTS

Fractional Denaturation as a Function of Temperature. The fractional populations of N, U, and D for the model

$$N \underset{k_2}{\overset{k_1}{\rightleftarrows}} U \xrightarrow{k_3} D$$

where $k_1 = 100v$ and for the two conditions $k_1 = k_3$ and $k_1 = (5 \times 10^4)k_3$ are given in Figure 1. This illustrates the dependence of the population values on the ratio of k_1/k_3. The temperature dependence of reversible unfolding and the irreversible step are highly dependent on the relative values of k_1, k_3, and v. When the forward rate constant for the reversible step is of similar magnitude to that for the irreversible step ($k_1 \simeq k_3$), denaturation is almost completely irreversible at all levels of unfolding. This is shown by the low concentration of reversible intermediate U present at any temperature. However, when the irreversible step is much slower [$k_3 = k_1/(5 \times 10^4)$], unfolding is nearly totally reversible until temperatures of 32–33 °C, the point at which 70–80% of the protein is unfolded.

Curves of this sort were generated for a wide range of values of k_1, k_3, and v, and dN/dT was calculated, which is proportional to C_p if the heat absorbed during the reversible step is much greater than that for the irreversible step. The remainder of this work deals with an analysis of these curves. The shapes of N, U, D, and C_p as a function of temperature are dependent on the ratios v/k_1 and v/k_3, where increasing values of v/k_i can be interpreted as increasing scan rate or decreasing rate constant. The use of these reduced variables is the most general way of presenting the final results. The relevant variable for reversible or irreversible two-state denaturation is v/k_1.

Two-State Irreversible Denaturation. The simplest kinetic model is for irreversible denaturation ($N \xrightarrow{k_1} D$). The curves of C_p vs T ($-dN/dT$ vs T) are shifted to higher temperature with increasing v/k_1 (Figure 2). This illustrates the importance of varying the scan rate or the rate of irreversible unfolding on the profiles. The profiles in Figure 2 cover a range of v, or alternatively k_1, of 6 orders of magnitude. The temperature of maximum C_p (T_{max}) obeys the relation

$$\frac{vE}{RT_{max}^2} = e^{A - E/RT_{max}}$$

(results not shown) as previously predicted (Sánchez-Ruiz et al., 1988). The apparent transition temperature (T_{app}, temperature at which N equals half its initial value) as a function of v/k_1 is given in Figure 5 by the curve labeled I. Denaturation is kinetically limited at all scan rates and for all values of the rate constant (k_1) for irreversible unfolding.

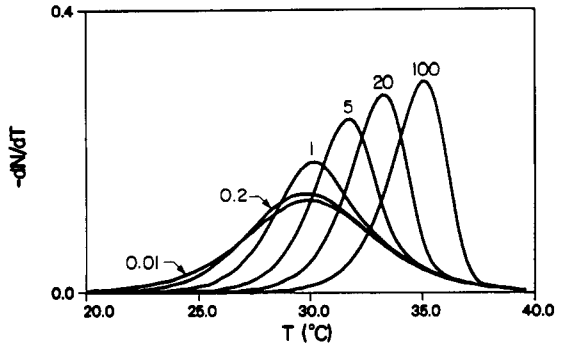

FIGURE 3: DSC profiles for two-state reversible denaturation for v/k_1 = 0.01–100 at 30 °C.

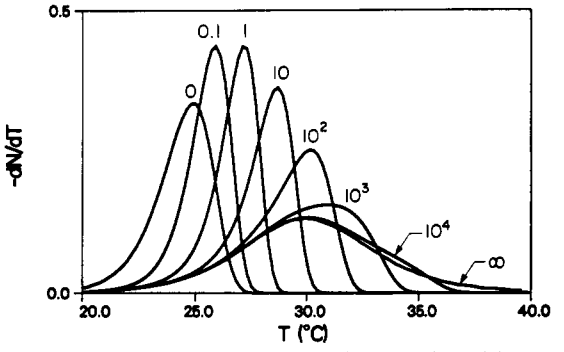

FIGURE 4: DSC profiles for three-state denaturation with constant k_1 (v/k_1 = 0.01 at 30 °C) and varying k_3 values, giving k_1/k_3 ratios of 0 (equivalent to irreversible two-state denaturation), 0.1–10 000, and ∞ (equivalent to reversible two-state denaturation).

Two-State Reversible Unfolding. The DSC profiles for reversible unfolding

$$N \underset{k_2}{\overset{k_1}{\rightleftarrows}} U$$

as a function of v/k_1 are shown in Figure 3, and T_{app} is given in Figure 5 by the curve labeled R. This illustrates how the profiles change when the scan rate or the rate of unfolding is varied. For scan rates much less than the rate of unfolding ($v/k_1 < 0.1$), N and U are in kinetic equilibrium and $T_{app} = T_m$. At $v/k_1 \gtrsim 0.1$, T_{app} begins to increase and merges with the values of T_{app} for irreversible denaturation at $v/k_1 \gtrsim 10$. For scan rates (or values of k_1) at which N and U are in equilibrium, the DSC profiles is slightly skewed to the high-temperature side which follows from the van't Hoff equation. At larger v/k_1, the curve shape becomes more like that for irreversible denaturation since unfolding is kinetically limited by k_1, with very little refolding occurring during the scan. Thus, for $v \gg k_1$ at T_m, the shape of the denaturation profile is determined almost totally by the forward, unfolding reaction. Thus, the apparent transition temperature for completely reversible unfolding can have a scan rate dependence when the scan rate exceeds the rate of unfolding.

Three-State Denaturation. The complete results for the three-state model

$$N \underset{k_2}{\overset{k_1}{\rightleftarrows}} U \xrightarrow{k_3} D$$

are more complicated to present since both k_1 and k_3 can vary. Profiles as a function of v/k_3 with v/k_1 = 0.01, selected so that the first step would be in equilibrium if denaturation was reversible, are shown in Figure 4. This illustrates how the profiles change when the scan rate or the rate of the irreversible step is varied. The value of v/k_1 = 0.01 is used in many of the following examples to simplify the analysis.

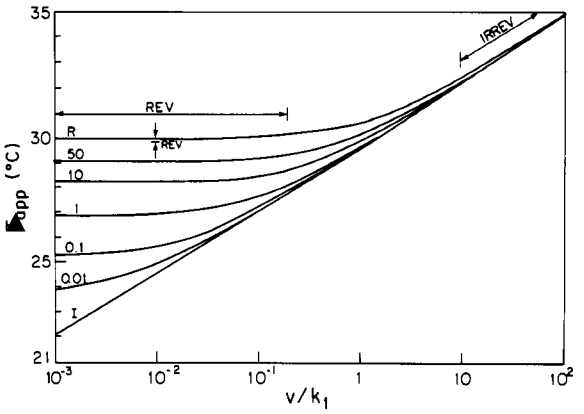

FIGURE 5: Apparent transition temperatures (T_{app}) as a function of v/k_1 for irreversible two-state denaturation (I), reversible two-state denaturation (R), and three-state denaturation (k_1/k_3 = 0.01, 0.1, 1, 10, and 50).

For $k_1/k_3 \gtrsim 10^6$, the DSC profiles are indistinguishable from the reversible case since no buildup of D occurs until N is completely unfolded. As k_3 increases, significant deviation from true reversibility occurs, which can be seen by comparing the reversible curve ($k_1/k_3 = \infty$) to $k_1/k_3 = 10^4$ in Figure 4. As k_3 increases further, the profile shifts to lower temperatures and becomes indistinguishable from totally irreversible denaturation at $k_1/k_3 \lesssim 10^{-4}$. At intermediate values of k_1/k_3 (e.g., 1000), the shape of C_p vs T is complex and has the appearance of consisting of more than one component.

Profiles of C_p vs T were generated at constant v/k_3 as a function of v/k_1, as was done in Figures 2 and 3, and the resulting T_{app}'s are given in Figure 5 for several values of k_1/k_3. A series of curves result that are bounded by the curves for reversible and irreversible denaturation. As k_1/k_3 increases (i.e., the rate of the irreversible step decreases with respect to the reversible step), the curve of T_{app} vs v/k_1 shifts from more irreversible to more reversible. Each curve, except that for true two-state irreversibility, has a plateau region at low v/k_1 where T_{app} is independent of v/k_1 (i.e., independent of scan rate). At greater values of v/k_1 corresponding to fast scan rates, the curves become similar and effectively merge at $v/k_1 > 10$. Thus, a region exists for each curve, even when denaturation is highly irreversible, where T_{app} is independent of scan rate. For example, for $k_1/k_3 = 1$, unfolding is nearly completely irreversible at all values of v/k_1, but T_{app} is constant and independent of scan rate as long as $v/k_1 < 0.01$. Thus, lack of a scan rate dependence for T_{app} is not a sufficient condition for deciding if reversible modeling is justified.

Curve Fitting. A major question is the following: What is the range of values of k_1, k_3, and v over which reversible curve fitting and deconvolution can be used to extract meaningful thermodynamic information from DSC profiles of C_p vs T? This question is relevant to any means of measuring denaturation by thermal analysis, not only DSC. This was determined by fitting the simulated profiles with the van't Hoff equation to obtain the best-fit values of ΔH_{app}, ΔS_{app}, and T_{app} for the reversible step. These were then compared to the actual values used in the simulation.

Shown in Figure 6 are the simulated profiles and best fits for k_1/k_3 = 2000 and 50 000 to illustrate this procedure. A reasonably good fit is obtained at k_1/k_3 = 50 000, but the fit degenerates severely at k_1/k_3 = 2000. Figure 7 gives ΔH_{app} obtained from the fits as a function of k_1/k_3. At large values of k_1/k_3, the fits are exact with the value of ΔH_{app} obtained from the best fit equal to the value used in the simulation (400 kJ/mol). As k_1/k_3 decreases (i.e., the rate of irreversibility

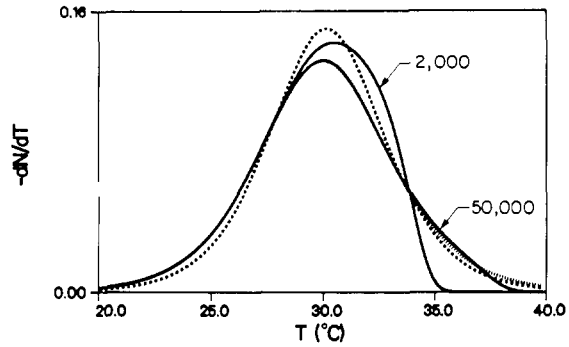

FIGURE 6: Best reversible curve fits for three-state denaturation ($v/k_1 = 0.01$) for $k_1/k_3 = 2000$ (dotted line) and $k_1/k_3 = 50\,000$ (dashed line). The simulated curves are given by the solid lines and labeled with the value of k_1/k_3.

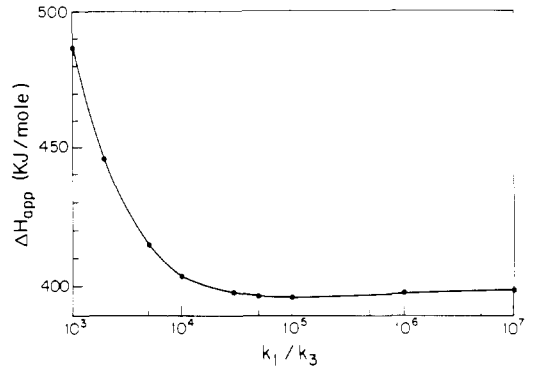

FIGURE 7: Apparent enthalpy ΔH_{app} (obtained from reversible curve fitting) as a function of k_1/k_3 for $v/k_1 = 0.01$.

increases), the quality of the fit decreases. The fit for $k_1/k_3 = 50\,000$ (Figure 6), which gives an ΔH_{app} that differs by about 1% from the true value, appears to be the worst acceptable for accurate fitting of high-quality DSC profiles. The fit for $k_1/k_3 = 2000$ (Figure 6) gives an ΔH_{app} that deviates from the actual ΔH by about 10%. This is a reasonably accurate determination of ΔH, but the quality of the fit judged by eye is very poor and totally unsuitable for purposes of deconvolution of multitransition profiles. As can be seen from Figure 7, there is a very sharp increase in ΔH_{app} as k_1/k_3 decreases below 10 000.

An additional problem in extracting thermodynamic information from curves with a shape similar to that for $k_1/k_3 = 2000$ is that the profile suggests the presence of more than one component. This can lead to the assumption of multiple or sequential transitions and an attempt at deconvolution into at least two components, resulting in an erroneous interpretation of the data.

Since k_1/k_3 is usually not known, the above analysis offers little practical help in deciding if a reversible analysis is suitable. However, in principle an approximate value of k_1/k_3 can be determined from the extent of irreversible denaturation as a function of the extent of unfolding. These curves were generated by calculating $N(T)$ and $D(T)$ throughout the temperature range of the DSC profile and are given in Figure 8 for $k_1/k_3 = 10^{-4}$–10^6. The value of v/k_1 was held constant at 0.01, and v/k_3 varied from 10^{-2} to 10^4. The curve for reversible denaturation is a straight line along the horizontal axis ($D = 0$ at all levels of unfolding), while that for irreversible denaturation is a straight line with a slope of 1 ($D = 1 - N$). For $k_1 < k_3$, denaturation is nearly completely irreversible at all points through the profile of C_p vs T. For $k_1 \gg k_3$, very little irreversible denaturation occurs until nearly all the protein is unfolded. For example, at $k_1/k_3 = 2000$, the minimum

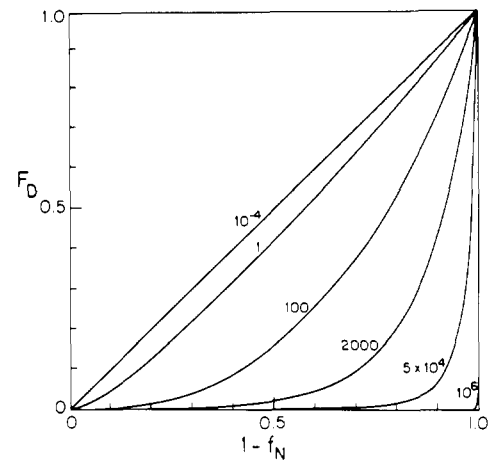

FIGURE 8: Fractional irreversible denaturation (D) as a function of fractional unfolding ($1 - N$) at k_1/k_3 ratios of 10^{-4}–10^6.

value for extracting useful thermodynamic information from a single-component profile as shown in Figure 6, about 2% and 14% irreversible denaturation occur at 50% and 75% unfolding, respectively. For the more conservative value of $k_1/k_3 = 50\,000$ for accurate curve fitting and deconvolution, virtually zero and about 1% irreversible denaturation occur at 50% and 75% unfolding, respectively. However, irreversibility is 100% for both cases at 100% unfolding. Thus, a high level of irreversibility can be tolerated at a high level of unfolding, but the formation of significant amounts of irreversibly denatured species in regions of the profile of C_p vs T that influence fitting perturbs the shape of the curve of N vs T, and hence C_p vs T, and influences the values of ΔH_{app} and ΔS_{app} obtained by curve fitting for reversible unfolding.

An approximate value of k_1/k_3, giving some idea of the rate of irreversibility, can be obtained by comparison of experimental curves of fraction irreversibly denatured (D) vs fraction unfolded ($1 - N$) to the theoretical plots shown in Figure 8. This would require determining the amount of irreversibility as a function of $N(T)$ in order to generate curves of the type shown in Figure 8. The experimental curves can then be compared to the theoretical curves to determine the ratio k_1/k_3. The exact shapes are determined by the actual activation energies E_1 and E_3 which would ordinarily not be known. Thus, the accuracy using this approach would not be great, but this is a very simple method for obtaining an approximate value of k_1/k_3 if even rough estimates for E_1 and E_3 can be obtained. An advantage of this approach is that it does not require varying the scan rate.

DISCUSSION

Several implicit assumptions are involved in the kinetic model of denaturation presented here:

(1) The protein goes through only three distinct conformational states for the three-state model and two for the simple reversible and irreversible models. The concentrations of any other intermediates are small compared to N, U, and D. Even for small globular proteins, some intermediates exist between the native and unfolded states (Privalov, 1979), and each macrostate N, U, and D is an ensemble of microstates (Biltonen & Freire, 1978); however, inclusion of these points would alter none of the final conclusions presented here although the curve profiles would be affected.

(2) The rate of transition between these states is limited by the free energy of activation (ΔG^*), which is determined by the conformation of the transition state, and the transitions

between states are pseudo-first-order. Treating the transitions as first order is clearly an approximation if additional folding intermediates exist. In addition, if irreversibility is due to aggregation, this step would be expected to be greater than first order.

(3) ΔH and ΔS for the reversible step are independent of temperature, which follows from the Arrhenius temperature dependence of the rate constants.

(4) All the absorption of heat occurs during the reversible step, except for the two-state irreversible model. Thus, all alterations in C_p vs T are due to a perturbation of population states, not an additional enthalpy of transition due to aggregation or any other process resulting in irreversible unfolding. The profile of C_p vs T would be altered even more from the reversible profile if irreversibility proceeds with a significant change in heat absorption or release. This is the case for a number of proteins including hemoglobin denaturation at high concentration where unfolding is followed by irreversible aggregation which has a calorimetric enthalpy approximately 25% that of unfolding (Lepock et al., 1989). Thus, the final restrictions on k_1/k_3 and the permitted fraction of irreversibility for a reversible analysis should be even stricter if the irreversible step has a significant enthalpy associated with it.

(5) The system is at temperature equilibrium. A method has been described to correct for the calorimeter response of existing calorimeters which results in minor deviations from equilibrium at the fastest scan rates presently used (Mavorga & Freire, 1987). However, no calorimeters have the ability to remain at temperature equilibrium while varying the scan rate by the several orders of magnitude necessary to distinguish between the two-state and three-state irreversible models and to determine k_1 and k_3 accurately.

Curves of the fractional populations of N, U, and D as a function of temperature for the model

$$\mathrm{N} \underset{k_2}{\overset{k_1}{\rightleftarrows}} \mathrm{U} \xrightarrow{k_3} \mathrm{D}$$

as a function of k_1, k_3, and v were generated. The DSC profiles (C_p vs T) were determined by differentiation of $N = N(T)$. T_{app} was calculated and the results given in Figure 5. One question that emerges is where on these curves do normal, DSC experiments fall.

The relaxation time (inverse of $k_1 + k_2$) for the reversible unfolding of ribonuclease A is approximately 20 s at T_m (Mayorga & Freire, 1987). This implies that $k_1 = k_2 \sim 0.02$ s^{-1} at T_m which gives $v/k_1 \sim 0.8$ at a scan rate of 60 °C/h, a commonly used value. This is slightly outside of the range of scan rates for which true equilibrium exists between N and U (Figure 5), which is also shown by the shift in T_{app} observed between $v = 10$ and 90 °C/h (Mayorga & Freire, 1987). The relaxation time of 0.4 s for the intermediate phase of unfolding of ribonuclease, which dominates the excess C_p profiles at T_m, is somewhat shorter (Freire et al., 1990), giving $k_1 \sim 1$ s^{-1} and $v/k_1 \sim 0.02$ at a scan rate of 60 °C/h. This is within but near the high end of the range of equilibrium. Thus, slow scan rates are needed to ensure equilibrium even for small, globular proteins. Values of ΔH_{app} within 10% of the true value are obtained by curve fitting only for $v/k_1 < 0.2$ (results not shown). This region of the reversible curve (R) is labeled REV in Figure 5.

Unfolding and refolding of domains in more complex large proteins and multisubunit proteins should proceed even slower. The trimeric tailspike endorhamnosidase of phage P22 unfolds through two steps in 2% SDS at 65 °C with rate constants of 1.1×10^{-3} and 4.0×10^{-5} s^{-1} (Chen & King, 1991). The slower rate constant gives a v/k_1 of 400 at a scan rate of 60 °C/h, which is well out of the region of reversible equilibrium. Thus, lack of equilibrium of native and unfolded species should be eliminated as a possible cause for an asymmetrical profile as shown in Figure 3 before a reversible analysis is used.

At large v/k_1, equivalent to very fast scan rates, denaturation is dominated by the forward reaction with little refolding during the course of the transition even for reversible unfolding. Thus, the rate of unfolding (k_1) and its temperature dependence (E_1) can be obtained by following unfolding at relatively high scan rates. Curve fitting assuming irreversible unfolding ($\mathrm{N} \xrightarrow{k_1} \mathrm{D}$) in the region $v/k_1 \gtrsim 10$, labeled IRREV in Figure 5, gives k_1 and E_1 for unfolding since very little refolding occurs in this region. The kinetics of refolding can then be obtained from a normal reversible analysis at $v/k_1 \lesssim 0.1$, where the native and unfolded species are in equilibrium. This is an alternative approach to obtaining relaxation times from the scan rate dependence of T_{app} (Mayorga & Freire, 1987) or multifrequency calorimetry (Freire et al., 1990). This approach is very simple and capable of a complete kinetic description; however, a calorimeter capable of scanning at rates varying by at least 2 orders magnitude is needed, which exceeds the capability of present instrumentation.

Introduction of a second, irreversible step following reversible unfolding always lowers T_{app} of the reversible step. The curves of T_{app} vs v/k_1 are bounded by the reversible curve for $k_1 \gg k_3$ and the irreversible curve for $k_1 \ll k_3$. Intermediate values of k_3 give curves with T_{app} independent of scan rate for small v/k_1 (shown by the plateau regions in Figure 5); however, denaturation is still irreversible. Thus, a lack of dependence of T_{app} on scan rate is not a sufficient condition for reversibility over the temperature range of the transition. The DSC profiles in these plateau regions of constant T_{app} are still highly perturbed by the irreversible step. The range of values of v/k_1 and k_1/k_3 for which a reversible analysis is appropriate is marked REV in Figure 5. This is a small subset of all possible values of k_1 and k_3.

In addition, a dependence of T_{app} on scan rate is not a sufficient condition for assuming irreversibility. Scan rates exceeding the rate of reversible unfolding (k_1) give an identical dependence of T_{app} on v as for irreversible denaturation if the rate constant for irreversibility is the same as k_1. As discussed in more detail below, two conditions are necessary for a simple reversible analysis: (1) the lack of dependence of T_{app} on scan rate and (2) the lack of formation of sufficient irreversibly denatured species to perturb the shape of the DSC profile.

An equilibrium thermodynamic analysis has frequently been used to analyze protein denaturation exhibiting a high degree of irreversibility. However, for a growing number of proteins, including the Ca^{2+}-ATPase of sarcoplasmic reticulum, yeast cytochrome c oxidase, and yeast phosphoglycerate kinase, the extent of unfolding closely matches the extent of irreversible inactivation (Lepock et al., 1990a; Morin et al., 1990; Galisteo et al., 1991), implying that $k_3 \gtrsim k_1$ and very little of the reversibly unfolded intermediate is present at any time. This distorts the reversible curve shape producing DSC profiles of the type shown in Figure 2. Thus, as suggested by Galisteo et al. (1991), it is necessary to develop approaches to determine when a reversible equilibrium analysis is suitable and when an irreversible kinetic analysis is required.

Sturtevant (1987) has suggested that a reversible analysis is appropriate for an equilibrium dissociative process followed by an irreversible step for a level of irreversibility such that 75% of the irreversible species is found at 95% unfolding. This

is comparable to the level of irreversibility for $k_1/k_3 \sim 2000$ (Figure 8). However, a single value for irreversibility at a high level of unfolding is not a suitable practical guide for determining when a reversible analysis is appropriate since only a little more irreversibility is found for cases when it is entirely inappropriate [e.g., $k_1/k_3 = 100$ (Figure 6), which gives 90% irreversibility at 95% unfolding (Figure 8)]. Reversibility must hold over most of the temperature region of the DSC profile from which information is extracted. A better guide would be the level of irreversibility allowed at a lower level of unfolding. At $k_1/k_3 = 2000$ for the model presented here, an upper limit would be 15% irreversibility at 75% unfolding. A more conservative limit seems prudent since the irreversible fit at $k_1/k_3 = 2000$ is not very good (Figure 6) and any heat absorbed or released during the irreversible step will further perturb the shape of C_p vs T. In addition, for a series of sequential transitions, this limit on irreversibility applies only to the last step, reducing still further the irreversibility allowed by the fractional value of the last step. Thus, one must be very careful when applying a reversible analysis to a partially irreversible process, and it is probably wise to demonstrate that the curve shape is not overly distorted by the formation of excessive levels of irreversibly unfolded protein.

Sanchez-Ruiz (1992) has recently shown that the reversible DSC profile can be altered by an irreversible step and that accepted tests for the applicability of a reversible analysis for multimeric proteins and ligand binding proteins do not always hold. The model used for irreversible denaturation

$$N \overset{K_{eq}}{\rightleftarrows} U \overset{k}{\rightarrow} D$$

is partially kinetic, but the first step is treated using equilibrium thermodynamics rather than rate constants. This model is equivalent to the full kinetic model used in this work as long as the scan rate is no more than one-tenth the rate of unfolding. Even for the small protein ribonuclease, this only holds for scan rates less than 1 °C/min. The predictions of the partially kinetic model used by Sanchez-Ruiz deviate from those of the full kinetic model for $v/k_1 \gtrsim 0.1$ (results not shown).

The formation of any irreversible component will alter the shape of C_p vs T over the temperature range at which it forms. Thus, some improvement in the accuracy of the thermodynamic parameters obtained by curve fitting will result if the high-temperature regions of C_p vs T where irreversibility becomes significant are not used for fitting. This approach requires that the number of transitions be known and that there be sufficient information in the remaining portion of the curve to accurately predict the shape of the profile at high temperatures.

In principle, it is possible to obtain the values of k_1, k_2, and k_3 and their temperature dependence by curve fitting and an analysis of T_{app} as a function of scan rate. The profiles of C_p vs T are totally determined by k_1 and E_1 at high scan rates. The values of k_2, k_3, E_2, and E_3 can be determined by the curve shape as a function of v (Figure 5) and the extent of irreversibility (Figure 8). However, this would require scan rates ranging over 2–4 orders of magnitude, depending on the values of k_1 and k_3, which are not achievable with presently available high-resolution scanning calorimeters.

A kinetic analysis of protein denaturation also illustrates the importance of kinetic factors, specifically the rate of the irreversible step, in determining the resistance of proteins to thermal inactivation. This is more important than conformational stability as characterized by T_m. We have shown that amino acid substitutions that reduce the T_m of denaturation of both bovine and human superoxide dismutase increase thermal stability if they reduce the rate of the irreversible step (McRee et al., 1990; Lepock et al., 1990b). Thus, it is possible to reduce conformational stability and increase thermal stability simultaneously. This approach for improving thermal stability should be applicable to other proteins.

REFERENCES

Biltonen, R. L., & Freire, E. (1978) *CRC Crit. Rev. Biochem. 5*, 85–124.

Brandts, J. F. (1964) *J. Am. Chem. Soc. 86*, 4291–4301.

Brandts, J. F., Hu, C. Q., Lin, L.-N., & Mas, M. T. (1989) *Biochemistry 28*, 8588–8596.

Chen, B., & King, J. (1991) *Biochemistry 30*, 6260–6269.

Dill, K. A., Alonso, D. O. V., & Hutchinson, K. (1989) *Biochemistry 28*, 5439–5449.

Edge, V., Allewell, N. M., & Sturtevant, J. M. (1988) *Biochemistry 27*, 8081–8087.

Freire, E., van Osdol, W. W., Mayorga, O. L., & Sánchez-Ruis, J. M. (1990) *Annu. Rev. Biophys. Biophys. Chem. 19*, 159–188.

Fujita, S. C., Gō, N., & Imahori, K. (1979) *Biochemistry 28*, 24–28.

Galisteo, M. L., Mateo, P. L., & Sanchez-Ruiz, J. M. (1991) *Biochemistry 30*, 2061–2066.

Kidokoro, S.-I., & Wada, A. (1987) *Biopolymers 26*, 213–219.

Lepock, J. R., Frey, H. E., Bayne, H., & Markus, J. (1989) *Biochim. Biophys. Acta 980*, 191–201.

Lepock, J. L., Rodahl, A. M., Zhang, C., Heynen, M. L., Waters, B., & Cheng, K.-H. (1990a) *Biochemistry 29*, 681–689.

Lepock, J. R., Frey, H. E., & Hallewell, R. A. (1990b) *J. Biol. Chem. 265*, 21612–21618.

Mayorga, O. L., & Freire, E. (1987) *Biophys. Chem. 87*, 87–96.

McRee, D. E., Redford, S. M., Getzoff, E. D., Lepock, J. R., Hallewell, R. A., & Tainer, J. A. (1990) *J. Biol. Chem. 265*, 14234–14241.

Morin, P. E., Diggs, D., & Freire, E. (1990) *Biochemistry 29*, 781–788.

Popescu, C., Segal, E., Tucsnak, M., & Oprea, C. (1986) *Thermochim. Acta 107*, 365–370.

Privalov, P. L. (1979) *Adv. Protein Chem. 33*, 167–241.

Privalov, P. L. (1982) *Adv. Protein Chem. 35*, 1–104.

Privalov, P. L. (1989) *Annu. Rev. Biophys. Biophys. Chem. 18*, 47–69.

Privalov, P. L., & Khechinashvili, N. N. (1974) *J. Mol. Biol. 86*, 665–684.

Privalov, P. L., & Filimonov, V. V. (1978) *J. Mol. Biol. 122*, 447–464.

Robert, C. H., Colosimo, A., & Gill, S. J. (1989) *Biopolymers 28*, 1705–1729.

Sanchez-Ruiz, J. M. (1992) *Biophys. J. 61*, 921–935.

Sanchez-Ruiz, J. M., López-Lacomba, J. L., Cortijo, M., & Mateo, P. L. (1988) *Biochemistry 27*, 1648–1652.

Sturtevant, J. M. (1987) *Annu. Rev. Phys. Chem. 38*, 463–488.

Tsalkova, T. N., & Privalov, P. L. (1985) *J. Mol. Biol. 181*, 533–544.

Zale, S. E., & Klibanov, A. M. (1986) *Biochemistry 25*, 5432–5444.